PRMT1-Mediated Metabolic Reprogramming Promotes Leukemogenesis

Hairui Su[1], Yong Sun[2], Han Guo[3], Chiao-Wang Sun[1], Qiuying, Chen[12], Szumam Liu[11], Anlun Li[11], Min Gao[4], Rui Zhao[1], Glen Raffel[5], Jian Jin[6], Cheng-qui Qu[7], Michael Yu[13], Christopher A. Klug[8], George Y. Zheng[9], Scott Ballinger[2], Matthew Kutny[10], X.Long Zheng[11], Zechen Chong[4], Chamara Senevirathne[3], Steve Gross[12], Yabing Chen[2]*, Minkui Luo[3,12]* and Xinyang Zhao[1,11]*

[1] Department of Biochemistry and Molecular Genetics, [2] Department of Pathology, [4] Department of Genetics, [8] Department of Microbiology, [10] Department of Pediatrics, The University of Alabama at Birmingham, School of Medicine, Birmingham AL 35294

[3]Tri-Institutional PhD Program in Chemical Biology; Chemical Biology Program, Memorial Sloan Kettering Cancer Center, New York, NY 10065

[5] Department of Medicine, University of Massachusetts, Cambridge, MA 02139

[6] Center for Therapeutics Discovery, Mountain Sinai Hospital, New York, NY USA

[7]Department of Pediatrics, Aflac Cancer and Blood Disorders Center, Children's Healthcare of Atlanta, Atlanta, GA 30322

[9] Department of Pharmaceutical and Biomedical Sciences, College of Pharmacy University of Georgia, Athens, GA 30602

[11]Department of Pathology & Laboratory Medicine, University of Kansas Medical Center, 3901 Rainbow Boulevard, Kansas City, KS 66160

[12]Program of Pharmacology, Weill Cornell Medical College of Cornell University, New York, NY 10021,

[13] Department of Biological Sciences, SUNY at Buffalo, Buffalo, NY

* Corresponding coauthors

Abstract:

Copious expression of protein arginine methyltransferase 1 (PRMT1) is associated with poor survival in many types of cancers, including acute myeloid leukemia. We observed that a specific acute megakaryocytic leukemia (AMKL) cell line (6133) derived from RBM15-MKL1 knock-in mice exhibited heterogeneity in Prmt1 expression levels. Interestingly, only a subpopulation of 6133 cells expressing high levels of Prmt1 caused leukemia when transplanted into congenic mice. The PRMT1 inhibitor, MS023, effectively cured this PRMT1-driven leukemia. Seahorse analysis revealed that PRMT1 increased the extracellular acidification rate (ECAR) and decreased the oxygen consumption rate (OCR). Consistently, PRMT1 accelerated glucose consumption and led to the accumulation of lactic acid in the leukemia cells. The metabolomic analysis supported that PRMT1 stimulated the intracellular accumulation of lipids, which was further validated by FACS analysis with BODIPY 493/503. In line with fatty acid accumulation, PRMT1 downregulated the protein level of CPT1A, which is involved in the rate-limiting step of fatty acid oxidation. Furthermore, administering the glucose analogue 2-deoxy-glucose (2-DG) delayed AMKL progression and promoted cell differentiation. Ectopic expression of Cpt1a rescued the proliferation of 6133 cells ectopically expressing PRMT1 in the glucose-minus medium. In conclusion, PRMT1 upregulates glycolysis and downregulates fatty acid oxidation to enhance the proliferation capability of AMKL cells.

Introduction:

Standard hematopoietic stem/progenitor cell transformation to AML cells requires metabolic reprogramming [1]. AML cells rely heavily on glucose for unchecked proliferation. Using ^{18}F-Fluoro-deoxy-Glucose (^{18}FDG) as a marker, Cunningham et al. detected high glucose uptake in the bone marrow of AML patients, and pyruvate and 2-hydroxy-glutarate concentrations negatively correlate with patient survival rates[2]. Dysregulated metabolic enzyme and mitochondria activities have been reported to be the causes of chemoresistance to AML [3,4] as well as solid tumors [5]. Metabolites such as acetyl-CoA, α-ketoglutarate, vitamin C (aka ascorbic acid), and *S*-adenosyl-L-methionine (SAM) are cofactors for histone and DNA modifications. Thus, metabolic reprogramming transforms the epigenetic landscape in leukemia cells. Mutations in isocitrate dehydrogenases, IDH1/2, produce 2-hydroxyl-glutarate (2-HG) instead of α-ketoglutarate. 2-HG inhibits demethylases that erase methylation marks on histones and DNA, and hydroxylases such as FIH (factor inhibiting HIF) in leukemia and glioblastoma [6]. However, mutations of metabolic enzymes in cancer are relatively rare. Usually, metabolic reprogramming is achieved mainly by expressing oncogenic transcription factors such as p53 mutants, HIF1, and FOXOs [7-10]. Dysregulation of signaling pathways such as KRAS mutations [5,11] and upregulation of the mTOR pathway during leukemogenesis [12] also alter metabolic pathways in tumorigenesis. Nevertheless, how epigenetic regulators involved in leukemogenesis regulate metabolic reprogramming still needs more research.

The protein arginine methyltransferase (PRMT) family has nine members, with PRMT1 responsible for most of the enzymatic activity in mammalian cells. PRMT1 is an epigenetic regulator via methylation of histone H4 and transcription factor RUNX1 [13,14]. The oncogenic roles of PRMT1 has been demonstrated in many types of solid cancers [15-24]. The importance of PRMT1 in leukemia has been shown in FLT3-ITD, AML1-ETO and MLL-EEN-associated acute myeloid leukemia and lymphoid leukemia [25-29]. Targeting PRMT1 is effective in treating leukemia with splicing factor mutations [30]. Yet, how PRMT1 is involved in cancer metabolic reprogramming has not been explored, albeit the known role of PRMT1 in metabolic regulation in model organisms. Phosphorylation of Hmt1 (PRMT1 ortholog in yeast) controls cell cycle progression in response to nutrition signals [31,32]. PRMT1 in *Caenorhabditis elegans and Trypanasome* is responsible for methylation of proteins inside mitochondria, although PRMT1 is not inside mitochondria, while PRMT1-null worms have dysfunctional mitochondria [33,34]. In Trypanosomes, PRMT1 promotes glycolysis and is required for virulent infection [35].

AMKL (acute megakaryoblastic leukemia) is a subtype of AML with leukemia cells stuck at the differentiation stage of immature megakaryocytes. AMKL is a rare leukemia often associated with Down syndrome. In cases not related to Down syndrome, AMKL is caused by chromosomal translocations.

Although AMKL can occur in adults, AMKL occurs more commonly in children [36]. Chromosomal translocation t(1;22) that generates RBM15-MKL1 fusion protein was discovered in childhood AMKL [37,38]. RBM15-MKL1 is a fatal disease without available targeted therapy.

Copious expression of PRMT1 is a poor prognostic marker for AML [39,40]. Furthermore, PRMT1 is expressed at an even higher level in AMKL than in other types of AML[40]. Constitutive expression of PRMT1 blocks terminal MK differentiation [40], while inhibition of PRMT1 activity promotes terminal MK differentiation[41]. Thus, we hypothesize that inhibiting PRMT1 activity could be a pro-differentiation therapy for AMKL. A leukemia cell line called 6133 is derived from Rbm15-MKL1 knock-in mice. When transplanted, 6133 cells can cause AMKL with low penetrance [42]. Using this leukemia mouse model; we report here that the elevated level of PRMT1 maintains the leukemic stem cells via upregulation of glycolysis and that leukemia cells with high PRMT1 expression are vulnerable to the inhibition of fatty acid metabolic pathways.

Results:

PRMT1 promotes the progression of RBM15-MKL1-initiated leukemia

The 6133 cells can be transplanted into recipient mice to induce low penetrant leukemia with symptoms closely recapitulating human AMKL[42]. To find additional factors needed to transform 6133 cells fully, we have reported a fluorescent probe (E84) that can be used to sort live cells according to PRMT1 protein concentrations [43] (Supplemental Figure 1). We sorted 6133 cells into two populations for bone marrow transplantation (BMT) according to E84 staining intensities (Figure 1A). All mice that received 6133 cells expressing higher levels of PRMT1 developed leukemia and died rapidly, while 6133 cells expressing lower levels of PRMT1 did not develop leukemia (Figure 1B). Consistently, a higher percentage of leukemia cells were detected in bone marrow and peripheral blood in recipient mice transplanted with E84-high (i.e., density staining of E84) 6133 cells according to FACS analysis (Figure 1C).

Given that E84-high cells can initiate leukemia, we introduced PRMT1 into 6133 cells (aka 6133/PRMT1 cells) using a lentivirus vector. Overexpression of PRMT1 rendered 6133/PRMT1 cells to increase in a cytokine-independent fashion in cell culture (Figure 1 D), and recipient mice transplanted with 6133/PRMT1 cells developed leukemia and died within 25 days (Figure 1 E&F). Although PRMT1-mediated methylation triggers the degradation of RBM15, PRMT1 overexpression does not affect the stability of the RBM15-MKL1 fusion (Supplemental Figure 2 A&B). The leukemic mice displayed splenomegaly. Intriguingly, the leukemia mice were paralyzed with observable spinal bleeding during dissection, although the bone density was still normal (data not shown). In a xenograft model with human RBM15-MKL1 leukemia cells, leukemia

also caused spinal bleeding [44]. Collectively, PRMT1 is required for the initiation of frank AMKL expressing RBM15-MKL1 fusion protein and leukemia initiated by 6133/PRMT1 cells in mice mimics several features of human AMKL.

MS023, a PRMT1 inhibitor, cures mice with Rbm15-MKL1-initiated leukemia

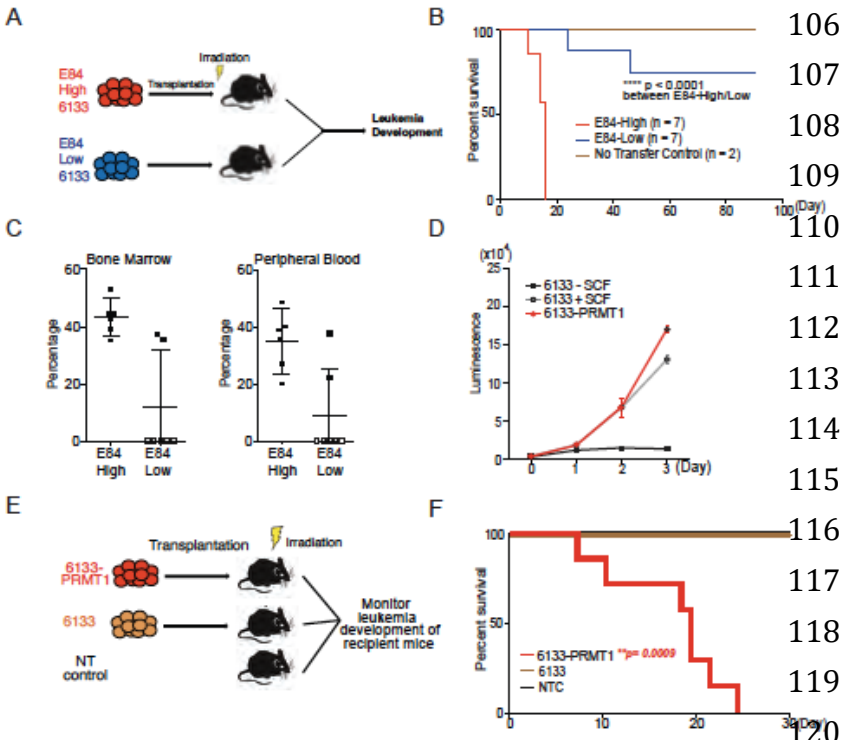

Figure 1. PRMT1 Promotes Leukemia Cell Transformation.
A. 6133 cells were stained with E84, then FACS was sorted based on E84 intensity. $3x10^5$ sorted cells were intravenously transferred to sublethally irradiated mice.
B. Leukemia progression in recipient mice was shown on Kaplan-Meier curves.
C. Leukemia cell manifestation in the bone marrow and peripheral blood of recipient mice was measured by flow cytometry. For the E84-low group, the bottom five dots represent five recipient mice sacrificed on day 90 post transfer. Closed symbols represent moribund mice, and open symbols represent non-terminally ill, inhibitor-treated mice sacrificed on day 88.
D. PRMT1 expression renders 6133 cells' cytokine-independent growth. 6133 cells and 6133/PRMT1 cells were cultured with or without mouse stem cell factor (SCF). Cell viabilities were measured daily.
E. Schematic for inducing leukemia by injecting 6133 or 6133/PRMT1 cells intravenously into sub-lethally irradiated recipient mice (n=7).
F. Leukemia progression in recipient mice was documented on Kaplan-Meier curves.

MS023 was reported to be a potent inhibitor of Type-I PRMTs including PRMT1 [41,45]. Furthermore, MS023 has been tested safe on mice at 80 mg/kg of body weight [29,41]. The 6133/PRMT1 cells were intravenously injected into sub-lethally irradiated recipient mice. A week after bone marrow transplantation (BMT), we injected intraperitoneally MS023 every other day for a month. Notably, while the mice in the untreated group exhibited rapid sickness and developed moribund symptoms, such as severe weight loss and rear limb paralysis, within 30 days, the majority of mice treated with MS023 remained healthy and symptom-free. MS023 treatment significantly alleviated leukemia burden, as shown by the FACS analysis of the percentages of leukemia cells in bone marrow and peripheral blood (Figure 2D). We also validated that the bone marrow cells from MS023-treated mice have reduced global levels of arginine methylation (Supplemental Figure 1C). Leukemia-associated splenomegaly was also relieved in MS023-treated mice (Figure 2D). Kaplan-Meir curves shew that the MS023-treated group was literally cured after

120 days (Figure 2C), with only residual leukemia cells detected in bone marrow and peripheral blood (Figure 2 D&E).

Expression of c-MPLW515L mutant in 6133 cells can render the 6133 cells fully penetrant for leukemia [42], and in vitro MS023 treatment reduced proliferation (Figure 2F). We then transplanted 6133/cMPLW515L cells into the congenic mice. In Figure 2 G-I, we demonstrated that MS023 also cures leukemia, which argues that PRMT1 can be a valid target for leukemia or myeloid proliferative disease driven by c-MPLW515L. Collectively, these data showed that PRMT1 is required to maintain Rbm15-MKL1-initiated leukemia in mice; targeting PRMT1 pharmacologically is an effective approach to treat leukemia.

PRMT1 promotes glycolysis in leukemia cells

Given that the role of PRMT1 in metabolic regulation has

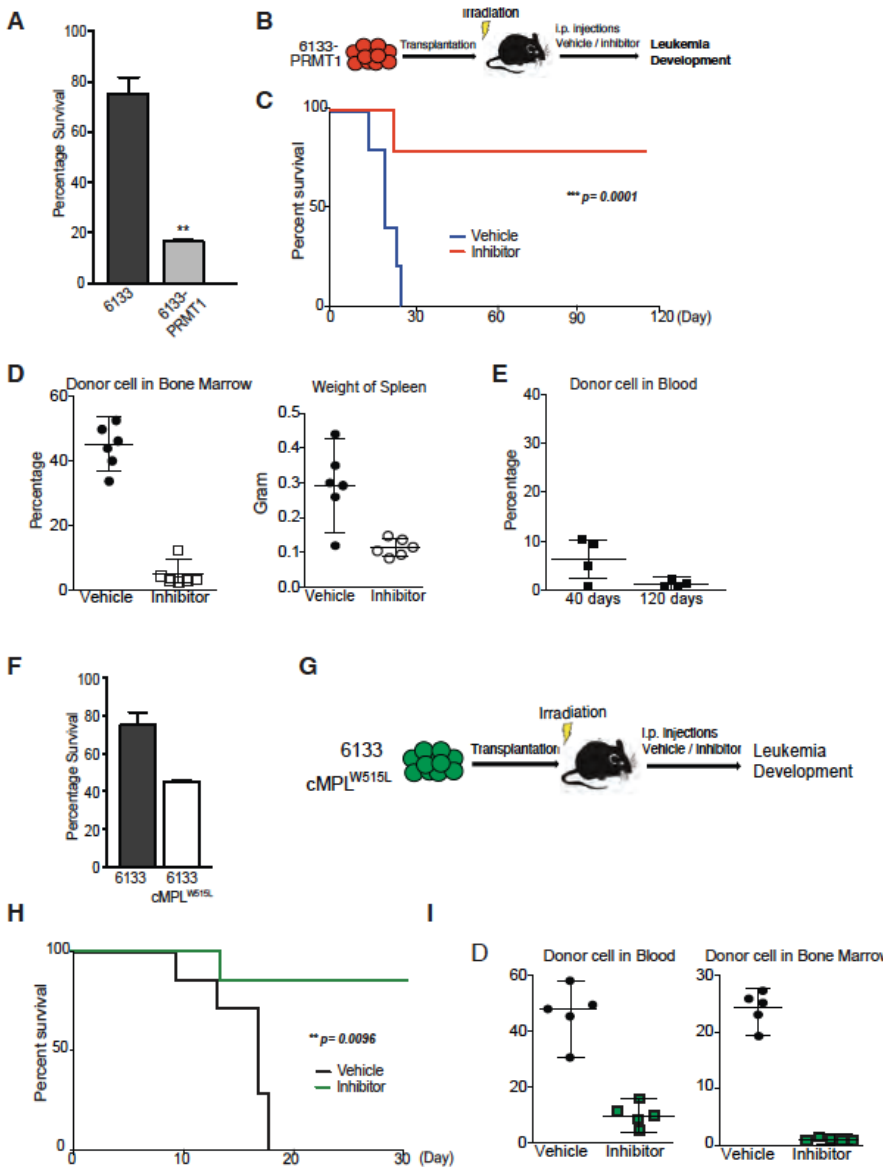

Figure 2. PRMT1 Inhibitor MS023 Blocks Leukemia Progression.
A. Survival of 6133/PRMT1 cell is highly sensitive to treatment of MS023. 6133 and 6133/PRMT1 cells were treated with MS023 for 48 hours and cell viability was determined by counting.
B. 6133/PRMT1 cells were intravenously transferred into sub-lethally irradiated Mice. Recipient mice were intraperitoneally injected with PRMT1 inhibitor or vehicle for 15 doses every other day.
C. Leukemia progression shown on Kaplan-Meier curves. n=5.
D. Leukemia cells in recipient mice (n=6) were measured by flow cytometry. The right panel indicates the weights of recipient mice spleens. Closed symbols represent moribund mice, and open symbols represent non-terminally ill, inhibitor-treated mice sacrificed on day 40 and 120.
E. Peripheral blood was collected from non-terminally ill, inhibitor-treated mice at 40 and 120 days post cell transfer.
F. MS203 treatment of in vitro cultured 6133 and 6133/cMPLW515L cells. n=3.
G. Schematic of leukemia induced by 6133 c-mplW515L transplantation.
H. Kaplan-Meier curves for MS023 treated leukemia mice induced by 6133 c-mplW515L cells. n=7.

been well-documented, we then investigated whether PRMT1 is involved in transforming 6133 cells through metabolic reprogramming. To assess this, we conducted Seahorse assays to measure the changes in ECAR (extracellular acidification rate) in 6133/PRMT1 cells compared to the parental 6133 cells. The ECAR curve of 6133/PRMT1 cells was elevated compared to that of 6133 cells (Figure 3A). Interestingly, the addition of FCCP, which uncouples oxidative phosphorylation from the TCA cycle, did not increase acidification levels.

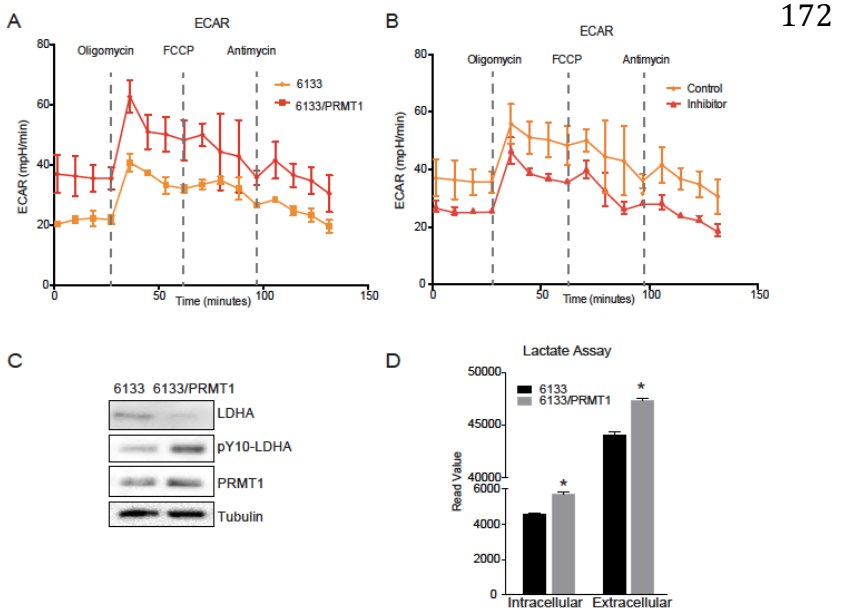

Figure 3. PRMT1 Promotes Glycolysis.
A. Extracellular acidification rates (ECAR) in 6133 and 6133/PRMT1 cells were measured by Seahorse assays. 150,000 cells were seeded in special 24-well plates for the Seahorse Xf-24 analyzer. Oligomycin, FCCP, and antimycin were sequentially injected into wells as indicated.
B. Extracellular acidification rates in PRMT1 inhibitor treated 6133 cells. Cells were pretreated with PRMT1 inhibitor MS023 overnight prior to Seahorse analysis.
C. Protein levels of lactate dehydrogenase A (LDHA) and p-Y10-LDHA in 6133 and 6133-PRMT1 cells by Western blotting. Cells were seeded in the same density and extracts were harvested after overnight culture.
D. Intracellular and extracellular lactate levels were measured by an L-lactate kit. Cells were seeded at $1x10^7$ cells/ml and cultured for 24 hours, followed by centrifugation. Both medium/supernatant (extracellular) and cell pellet (intracellular) were collected for analysis. The results of triplicates are plotted. * $p < 0.05$

Similarly, antimycin did not cause a significant drop in acid concentration. Remarkably, we treated 6133 cells with MS023 overnight prior to Seahorse assays and observed a reduction in ECAR levels (Figure 3B). These findings suggest that PRMT1 is responsible for the observed increase in acidification. In this

experiment, glycolysis contributes the most to acidification in the 6133 leukemia cells, as the addition of mitochondrial respiratory inhibitors only moderately reduces acidification levels according to the principles outlined by Divakaruni et. al. [46]. Lactate dehydrogenase A (LDHA), the final key enzyme in glycolysis that

converts pyruvate to lactate for NAD+ regeneration, was found to be influenced by PRMT1 overexpression. Specifically, PRMT1 overexpression stimulated the tyrosine phosphorylation of LDHA, thereby activating its enzymatic activity [47] despite an overall decrease in LDHA levels (Figure 3C). Consistently, when we directly

measured the intracellular and extracellular lactate levels of 6133 and 6133/PRMT1 cells, we observed that 6133/PRMT1 cells not only released more lactate into the medium but also had higher intracellular lactate

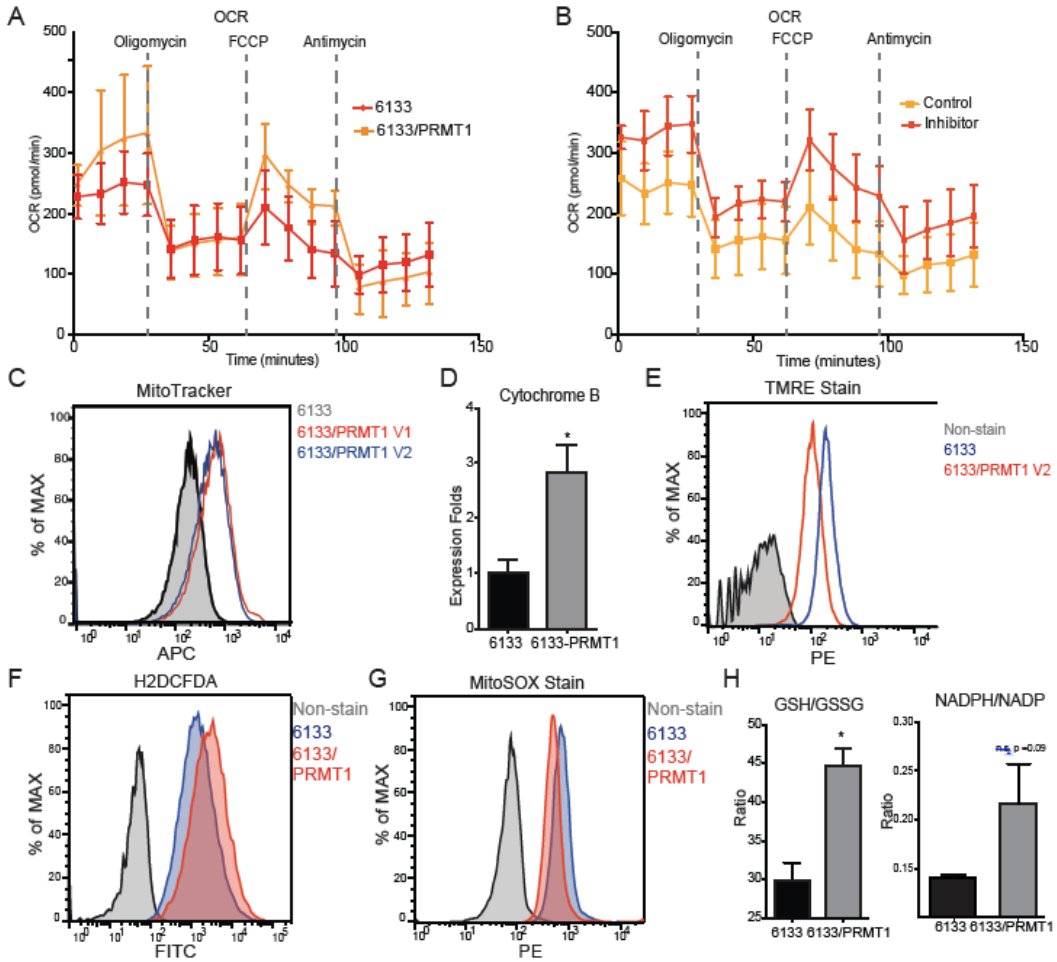

Figure 4. PRMT1 Changes Oxygen Consumption and Redox Status.
A. Oxygen consumption rates (OCR) in 6133 and 6133/PRMT1 cells were measured by Seahorse assays. 150,000 cells were seeded in special 24-well plates for Seahorse Xf-24 analyzer. Oligomycin, FCCP and antimycin were sequentially injected into wells as indicated.
B. Oxygen consumption rates in PRMT1 inhibitor-treated 6133 cells. Cells were pretreated with PRMT1 inhibitor MS023 overnight prior to Seahorse analysis.
C. Mitotracker Deep Red FM stain was used to assess the mitochondria mass in 6133 and 6133-PRMT1 cells.
D. Mitochondrial DNA amount was measured by quantitative PCR of mito-specific gene cytochrome B.
E. TMRE staining was performed to measure mitochondrial membrane potential. Cells were seeded at 1.1×10^5 cells/ml, and 0.1 volume of 5mM TMRE was added to the culture to reach a final concentration of 500nM. After 20 minutes, cells were collected and used for FACS analysis.
F. Intracellular ROS level was measured by H2-DCFDA staining. 1×10^5 cells were incubated in a warm staining solution containing 10 uM of H2-DCFDA for 30 minutes and then washed and subjected to analysis.
G. Mitochondrial ROS was measured by MitoSOX staining. 5x105 cells were incubated with a warm staining solution containing 2.5 uM of MitoSOX for 10 minutes and then washed and subjected to analysis.
H. Intracellular levels of GSH/GSSG and NADP/NADPH ratio were measured. In each assay, 5×10^5 cells were used for extract preparation.

levels (Figure 3D). We therefore concluded that PRMT1 promotes cellular glycolysis and lactate production, which predominantly contributes to the observed increase in acidification.

PRMT1 reduces oxygen consumption in mitochondria

The Seahorse assays have demonstrated that the cellular OCR (oxygen consumption rate) was reduced in 6133 cells. Additionally, it was observed that these cells had a limited capacity for reserve respiration, as the maximum respiration level was nearly identical to the basal OCAR level, regardless of the expression levels of PRMT1 (Figure 4A). Conversely, when the 6133/PRMT1 cells were pre-treated with MS023 overnight before the Seahorse assays, there was an increase in mitochondrial oxygen consumption compared to the non-treated controls (Figure 4B). These findings further support the notion that PRMT1 plays a role in mediating metabolic reprogramming by enhancing glycolysis and reducing mitochondrial oxygen consumption.

We have demonstrated that PRMT1 increases the number of mitochondria in MEG-01 cells, an acute megakaryocytic leukemia cell line (Zhang et al., 2015). In this experiment, FACS analysis with MitoTracker staining (Figure 4C) and real-time PCR analysis of mitochondrial DNA (Figure 4D) further validated that PRMT1 upregulated the mitochondria biogenesis in 6133 cells. H2DCFDA staining demonstrated that PRMT1 elevated global ROS levels in 6133 cells (Figure 4F). Intriguingly, when we performed Mito-Sox staining for ROS levels inside mitochondria, we found reduced levels of ROS (Figure 4G). The data implies that most of the ROS detected by H2DCFA may be generated from cytoplasm rather than from mitochondria, which is also agreeable with the Seahorse data that oxidation consumption in mitochondria is reduced (Figure 4A). Next, we performed TMRE staining for mitochondrial membrane potential. 6133/PRMT1 cells have reduced staining, which implies that PRMT1 reduces membrane potential (Figure 4E). This result also cross-validated the Seahorse findings that PRMT1 reduced mitochondrial oxygen consumption.

Given that the cytoplasmic ROS level was significantly raised upon PRMT1 expression, we measured the ratios of two redox pairs: glutathione and $NADP^+$. Intriguingly, activation of PRMT1 increased the ratios of both GSH/GSSG and $NADPH/NADP^+$. Given the essential roles of GSH and NAPDH in biomass synthesis, PRMT1 upregulation may support anabolism, consistent with PRMT1's role in supporting cell proliferation.

Metabolomic analysis of 6133/PRMT1 cells

To further probe the complexity of PRMT1-mediated metabolic reprogramming, we established a new 6133 cell line that can conditionally express PRMT1 upon adding doxycycline to the medium. We compared the metabolomic status of 6133 cells before and after 12 hours of PRMT1 induction. The cells were grown in standard RPMI1640 medium with 10% fetal bovine serum, with high concentrations of glucose and essential amino acids for 12-hour growth. We repeated the metabolomic analysis strictly five times. Principle core analysis indicated that PRMT1 caused a significant shift in metabolite profiles (Figure 5A,B).

Notably, PRMT1 activation led to increased ATP production and the accumulation of succinyl-CoA, alanine, serine, and short-chain fatty acids. Conversely, it resulted in a depletion of SAM, aspartic acid, nicotinamide,succinyl-homoserine, oxidized glutathione (which is consistent with the increased ratio of GSH/GSSG shown in Figure 4H), and alpha-ketoglutarate (aka oxoglutaric acid) (Figure 5C). These findings suggest that the beta-oxidation of fatty acids may be impaired, leading to the accumulation of fatty acids such as docosadiencic acid, caproic acid and suberic acid, while the levels of palmitoyl-carnitine are reduced. Furthermore, the reduced levels of alpha-ketoglutarate indicate potential alterations in the TCA cycle and glutaminolysis. Overall, our data highlights the profound metabolic changes induced by PRMT1, particularly in amino acid biosynthesis, one-carbon metabolism as shown in Figure 5D generated by the metaboAnalyst software [48].

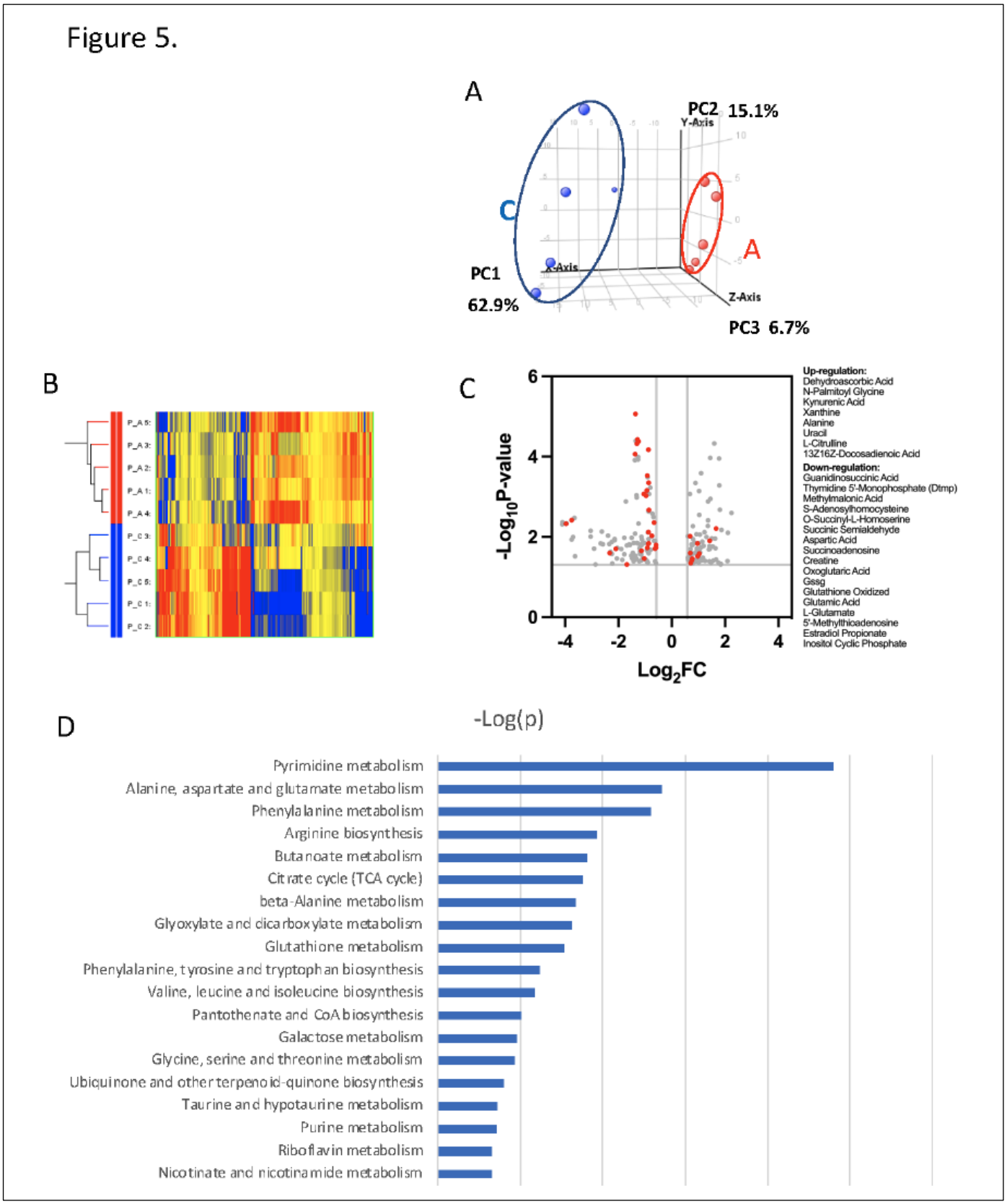

229 Figure 5: Metabolomic analysis of PRMT1-regulated metabolism in 6133 cells. 6133 cells expressing

doxycycline-inducible PRMT1 were induced to express PRMT1. The activated group (labelled as A): metabolites collected after PRMT1 was induced. Control group (labelled as C): metabolites collected before PRMT1 was induced.

A: principle component analysis (PCA) for the metabolites. The C group and A group were clustered at different positions in PCA analysis.

B: heatmap of metabolites differentially expressed in these two groups.

C: volcano plots for metabolites. 204 metabolites are changed more than 2 folds with $P < 0.5$.

D: Metabolic pathways are mostly affected by PRMT1 overexpression in 6133 cells. The metabolite data were analyzed by a web-based program called MetaboAnalystR6.0.

PRMT1-transformed leukemia cells are highly dependent on glucose consumption.

After determining that glycolysis was enhanced in PRMT1-overexpressing cells, we performed glucose colorimetric assays to measure the glucose concentrations in the cell culture medium when the 6133 and 6133/PRMT1 cells grew exponentially. More significant reduction of glucose in 6133/PRMT1 cells was observed than that in parental 6133 cells (Figure 6A), indicating that elevated glucose consumption via glycolysis is caused by PRMT1 upregulation. Next, we grew the cells both in glucose-containing and glucose-depleted media. Cell viability assays showed the slower growth of 6133/PRMT1 cells in a glucose-free medium, while the development of parental cells was less affected (Figure 6B). Accordingly, we used 2-deoxy-D-glucose (2-DG), a glucose analog that competes with glucose in glycolysis. The proliferation of 6133/PRMT1 cells was notably inhibited by 2-DG, while the proliferation of 6133 cells was barely affected (Figure 6C). These results are consistent with Seahorse analysis that 6133/PRMT1 cells rely on glycolysis for growth (Figure 3). Next, we tested whether glucose blockage can impede AMKL progression in mice. Four days after transplantation of the 6133/PRMT1 cells, we administered 2-DG to the mice at 0.5g/Kg body weight every other day for a month. 2-DG treatment significantly postponed disease progression (Figure 6D). The splenomegaly was alleviated, and the burden of leukemia cells in bone marrow and peripheral blood was notably decreased in 2-DG treated mice (Figure 6E&F). Taken together, the in vitro and in vivo data indicate that PRMT1-mediated metabolic reprogramming makes leukemia cells highly addicted to glucose.

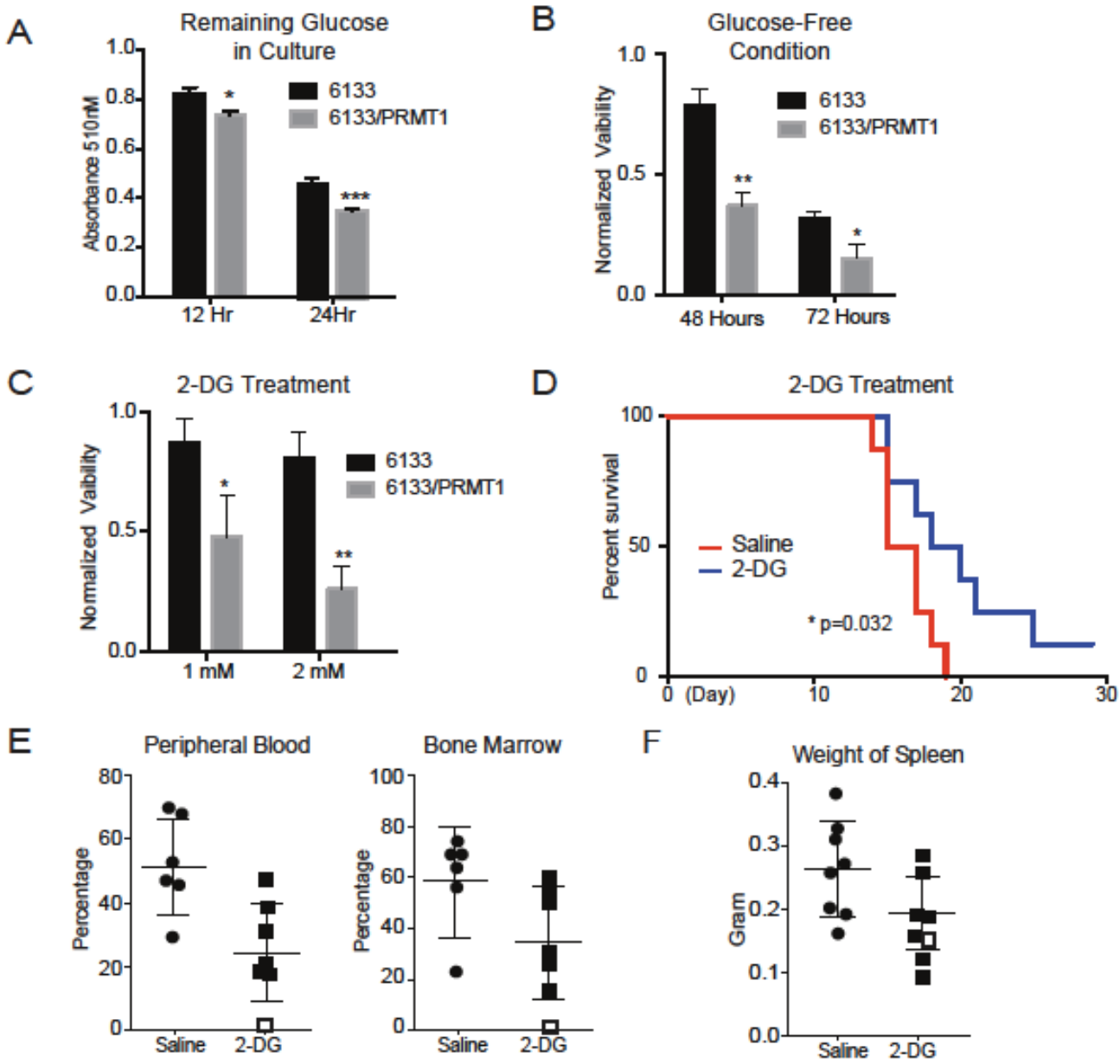

Figure 6. PRMT1 Causes Leukemia Cells' Heavy Dependency on Glucose consumption.
A. Glucose colorimetric assay of 6133 and 6133/PRMT1 cells. 1.25x 105 cells were seeded per well and cultured overnight. After centrifugation, supernatant/medium was collected and used for the assay.
B. Cell viability of 6133 and 6133/PRMT1 cells under glucose-free conditions. Cells were seeded in a 96-well plate with fresh regular or glucose-minus RPMI1640 medium. Cell viability was measured by CellTiter-Glo kit. Ratios were normalized to the wells with regular RPMI-1640 medium.
C. Cell viability of 6133 and 6133/PRMT1 cells with 2-DG treatment. Cells were seeded in 96-well plates supplemented with 2-DG. Cell viability was measured by CellTiter-Glo kit. The growth of cells without 2-DG addition was used for normalization.
D. 6133/PRMT1 cells were intravenously transferred into sub-lethally irradiated mice. Starting on day 4 post-transfer, recipient mice were intraperitoneally injected with saline or 0.25g/Kg body weight of 2-DG every other day. The survival of recipient mice is shown as Kaplan-Meier curves.
E. Percentages of leukemia cells in bone marrow and peripheral blood of recipient mice were measured by flow cytometry. Closed symbols represent mice transplanted with 6133/PRMT1 cell-induced leukemia. The open square is a control wild type mouse without leukemia.

258

Targeting fatty acid metabolic pathways for leukemia therapy

Rapidly growing cancer cells need de novo synthesis of fatty acids to meet the demand for building cell membranes [49]. De novo fatty acid synthesis uses acetyl-CoA generated from fatty acid oxidation. Inhibition of fatty acid oxidation has been shown to kill leukemia cells [50]. Carnitine-palmitoyl-transferase (CPT1A) catalyzes the rate-limiting step of fatty acid oxidation by transporting fatty acids across the mitochondrial outer membrane. RBM15 binds to 3'UTR of CPT1A mRNA (Zhang et al., 2015). Furthermore, PRMT1 controls the stability of the RBM15 protein. We demonstrated that the expression of both isoforms of PRMT1 lowered the mRNA levels of CPT1A (Figure 7A). We then performed Western blotting and confirmed that the protein level of CPT1A was accordingly reduced in 6133 cell lines ectopically expressing PRMT1 isoforms (Figure 6B). Downregulation of CPT1A causes less consumption of long-chain fatty acids. We consistently found more lipid accumulation in 6133/PRMT1 cells than in 6133 cells by FACS analysis with lipid-binding fluorescent dye (Figure 7C). Metabolomic analysis also found the accumulation of fatty acids such as suberic acid and caproic acid while downregulation of palmitoyl-carnitine which is a product of CPT1A (see supplemental table 1 for metabolomic data). We then treated leukemia cells with etomoxir, which inhibits CPT1A enzymatic activity. The 6133/PRMT1 cells were more sensitive to etomoxir than the 6133 cells (Fig 6D). Orlistat, a FASN inhibitor, also impeded the proliferation of 6133/PRMT1 cells more effectively than that of 6133 cells (Fig 6E). While CPT1A is responsible for transporting long-chain fatty acids, short-chain fatty acids can be directly transported to mitochondria. We added acetate, propionate, and butyrate in the form of triglycerides to a glucose-free medium. Strikingly, all three forms of short-chain fatty acids could support the proliferation of 6133/PRMT1 cells better than the parental 6133 cells (Fig 6F). The data implies that leukemia cells with high levels of PRMT1 expression can use short-chain fatty acids to compensate for the need for glucose.

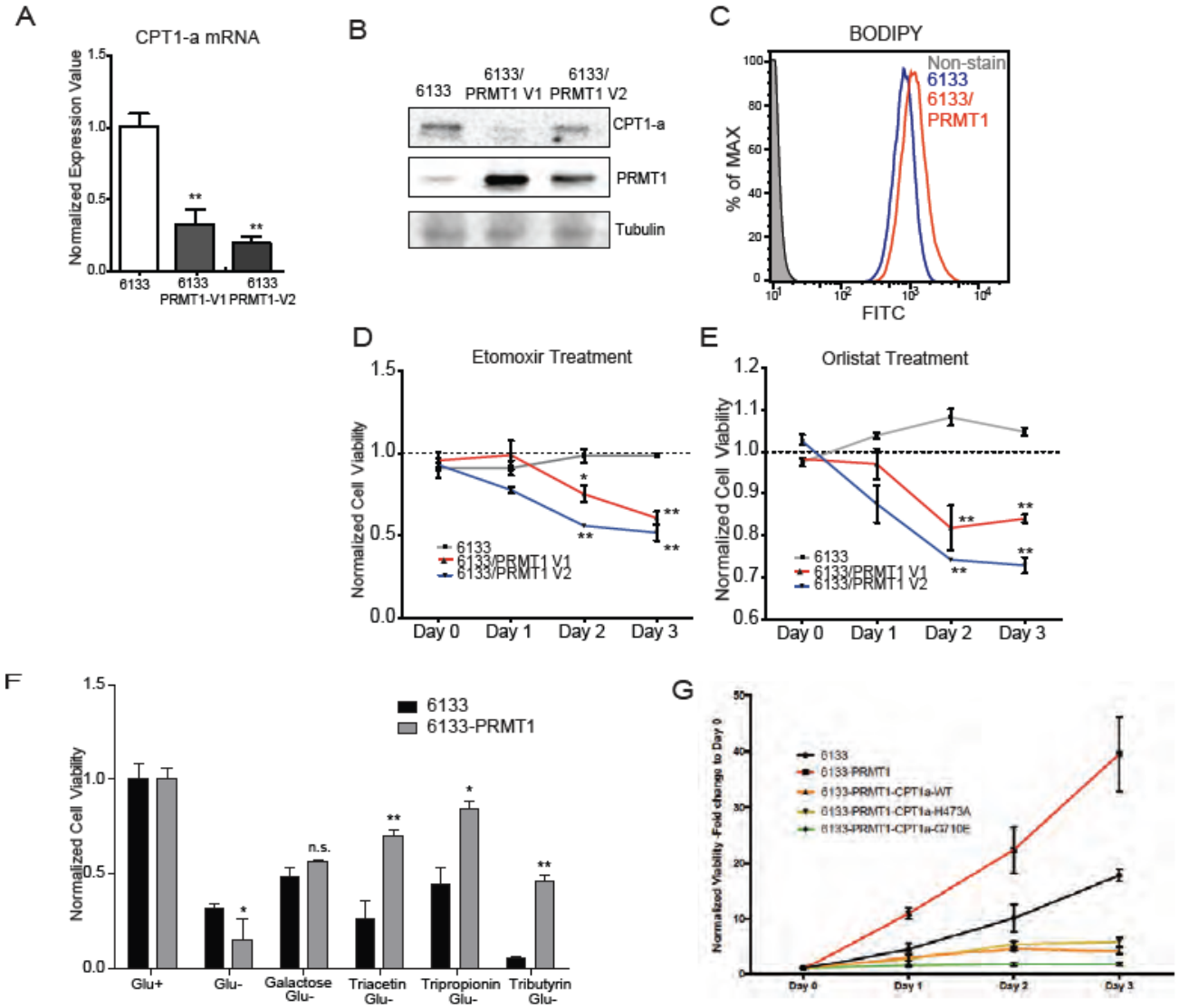

Figure 7. PRMT1 Alters Fatty Acid Oxidation in Leukemia Cells.
A. mRNA level of CPT1a and PPARα in 6133 and 6133-PRMT1 cells. Cell pellets were harvested in Trizol before RNA extraction, followed by cDNA synthesis and qPCR analysis.
B. Western blotting of 6133 and 6133-PRMT1 cell lines.
C. BODIPY Staining of 6133 cells. Cells were incubated with 200nM of BODIPY at 37oC for 15 minutes before being washed with medium and sent for FACS analysis.
D. Cell viability of 6133 and 6133-PRMT1 cells with Etomoxir treatment. 6133 and 6133-PRMT1 cells were seeded in a 96-well plate, supplemented with Etomoxir. Cell viability was measured by CellTiter-Glo Kit. Ratios were normalized to day 0.
E. Cell viability of 6133 and 6133-PRMT1 cells with Orlistat treatment.
F. Viability of 6133 and 6133-PRMT1 cells with a supplement of short-chain fatty acid (triacetin/ tripropoinin/tributyrin) under glucose-free conditions. Cells were cultured with RPMI with or without glucose, supplemented with 100nM of triacetin/tripropionin/tributyrin, respectively. Cell viability was measured after 72 hours. Fold change of viability is normalized to glucose+ cells.
G. Growth curves of 6133-PRMT1 cells transduced with CPT1A, CPT1A/H473A and CPT1A/G710E.

We then used a lentivirus to express CPT1A in 6133/PRMT1 cells ectopically. CPT1A wild type and mutant (H473A) that does not have succinylation activity [51] dampens the proliferation rates of 6133/PRMT1 cells grown in regular culture conditions. Intriguingly, the CPT1A enzymatic dead mutant (G710E) blocks the proliferation of the 6133/PRMT1 cells, which implies that the 6133 cells still need fatty acid oxidation for de novo synthesis of lipids for proliferation (Figure 7G). Taken together, we reveal that although PRMT1 downregulates fatty acid oxidation as an energy source, PRMT1 upregulates the usage of short-chain fatty acids as an alternative energy source for mitochondria.

Discussion:

This report demonstrated that PRMT1 expression is required for RBM15-MKL1-initiated leukemia in mice. Given that only leukemia cells expressing elevated levels of PRMT1 can cause leukemia (Figure 1) and that normal hematopoietic stem cells express low levels of PRMT1[43], targeting PRMT1 may spare the normal hematopoietic stem cells. Given the essential roles of PRMT1 in AML with wide range of gene mutations such as RBM15-MKL1, FLT3-ITD, MLL-EEN, and AML1-ETO fusions as well as AML with splicing factor mutations [30], the mechanism on how PRMT1 drives leukemia becomes particularly important to investigate further. Here, we demonstrated the critical regulation of metabolic pathways by PRMT1.

Many substrates of PRMT1 have been characterized, including metabolic enzymes such as GAPDH[52] and PHGDH[53] and regulators such as PGC1, FOXOs, and RBM15 [54]. PGC1 and FOXO1 are known regulators of metabolism [55,56]. RBM15 regulates hematopoietic stem cell homeostasis and megakaryocyte differentiation [57,58]. We demonstrated that almost 50% of RBM15 targets are metabolic enzymes whose 3'UTR regions on mRNAs are bound by RBM15[40]. The CPT1A mRNA is one of them. Since our metabolomic analysis demonstrated that PRMT1 overexpression caused the accumulation of intracellular lipids, we examined the CPT1A protein levels in the two cell lines. PRMT1 downregulates CPT1A protein level, which may partially explain lipid accumulation. Nevertheless, PRMT1 does not turn off TCA cycle or fatty acid oxidation, since the 6133/PRMT1 cells still support proliferation using galactose and glycerol in combination with acetate (triacetin), propionate (tripropionin) and butyrate (tributyrin) (Figure 7G). Transporting short-chain fatty acids across mitochondria does not require CPT1A expression. Thus, these molecules can be converted to acetyl CoA and propionyl-CoA and butyl-CoA to feed into TCA cycle. Although reduced oxygen consumption and membrane potential in mitochondria suggest the reduced activity of respiratory chain in mitochondria when long-chain fatty acids are supplied as fuels, the respiratory chain per se is still intact so the 6133/PRMT1 cells can adapt to the consumption of short chain fatty acid and non-fermentable carbon sources such as glycerol and galactose. We then rescued the growth of 6133/PRMT1 cells in a glucose-minus medium by ectopically expressing CPT1A, which argues

that CPT1A-mediated fatty acid oxidation is the major pathway regulated by PRMT1. RBM15 also binds to several mRNAs coding for enzymes involved in glycolysis: LDHA and HK1. Although we did not detect increased protein expression of HK1 and LDHA, we did observe the increase of tyrosine phosphorylation of lactate dehydrogenase A (LDHA) by PRMT1. Since phosphorylation activates LDHA, upregulation of PRMT1 activates glycolysis. The decreased ratio of NADP/NADPH reduces aspartate concentration, which is another strong indicator of prominent levels of glycolysis in proliferating cells[59,60]. Consistently, we also observed downregulation of aspartate as well as decreased ratio of NADP/NADPH in the 6133/PRMT1 cells. In conclusion, our data reveal the profound effect of PRMT1 upregulation on metabolic reprogramming.

Another intriguing phenomenon is that PRMT1 overexpression promotes mitochondria biogenesis as we reported before and further validated here (Figure 4C and D). However, the increase of mitochondria number did not translate to higher oxygen consumption. Actually, the ROS level inside mitochondria per cell is reduced, which is consistent with reduced membrane potential and lower oxygen consumption we observed. How PRMT1 regulates electron transportation chain at transcription and posttranscription levels needs more studies in the future. Intriguingly, we detected an increase of the total level of ROS, which implies that PRMT1 upregulates the ROS in the cytoplasm. Since lipids can stimulate the generation of ROS[61], we speculate that intracellular accumulation of lipids by PRMT1 may be responsible for ROS increase in the cytoplasm. We posit that in cancer cells expressing copious levels of PRMT1, the main function of mitochondria is to generate intermediate metabolites for biomass synthesis. Understanding how PRMT1 regulates metabolic pathways may open new therapeutic avenues for cancer and other chronic diseases such as diabetes.

Acknowledgement:

The project was partially supported by Leukemia Research Foundation to XZ, NCI R21 CA202390 to XZ, and Elsa Pardee Foundation to XZ. We would like to thank Dr. Taro Hitosugi (Mayo Clinic) for the CPT1A cDNAs.

Methods and Methods

<u>Cell Culture and metabolite measurement</u>

6133 cells were cultured in RPMI1640 medium supplemented with 10% FBS100 U/mL penicillin and 100 μg/mL streptomycin. Addition or withdrawal of mSCF (10 ng/mL) in culture were performed accordingly. L-

Lactate Assay Kit (Cayman, Ann Arbor, Michigan) was used to measure the intracellular and extracellular lactate levels of cultured cells: approximately $1x10^7$ cells were cultured in 10 mL fresh medium for 24 hours; cell pellet and medium were collected and processed separately as instructed. Glucose Colorimetric Assay Kit (Cayman, Ann Arbor, MI) was used to quality the remaining glucose in culture medium: $1.25x10^5$ cells were cultured in fresh medium overnight; supernatant/medium was collected and processed as instructed. The fluorescent or colorimetric signals of the assays above were measured using a microplate reader (Biotek, Winooski, VT).

Viral Production and Cell Line Selection

For lentivirus production, viral vectors were co-transfected with envelope vector pMD2.G and packaging vector ps-PAX2 into 293T cells. Fresh or concentrated viruses were used to infect target 6133 cell lines. Stable cell lines were selected via GFP-based flow-cytometry sorting by BD FACSAria II system (BD, Franklin Lakes, NJ).

Murine Leukemia Model and Treatments

GFP-positive 6133 cells were intravenously transferred into 8-12 weeks old sub-lethally irradiated (6 Gy) C57BL/6 mice. Disease progression was closely monitored on a daily basis. Moribund mice were sacrificed for further analysis of GFP-positive donor leukemia cells in peripheral blood, bone marrow, and spleen. For PRMT1 inhibitor treatment, 80 mg/Kg body weight of inhibitor solution (16 mg/mL) was intraperitoneally injected into recipient mice every other day for a month, starting from the fourth-day post-cell transfer. PRMT1 inhibitor was dissolved in saline with 20% Captisol, 20% PEG-400 and 5% NMP (v/v). For 2-DG treatment, 0.25 g/Kg body weight of 2-DG (saline solution) was intraperitoneally injected into recipient mice every other day for a month, starting the fifth-day post cell transfer.

Flow Cytometry Analysis

FACS analysis was performed on BD LSRFortessa (BD, Franklin Lakes, NJ). Mitotracker DeepRed FM stain and TMRE stain (Molecular Probes, Eugene, OR) were used to assess cellular mitochondria.

SDS-PAGE and Western Blotting

6133 cells were collected from culture and lysed in 1 mL H-Lysis buffer (20 mM HEPES pH 7.9, 150 mM NaCl, 1 mM $MgCl_2$, 0.5% NP40, 10 mM NaF, 0.2 mM $NaVO_4$, 10 mM β-glycerol phosphate and 5% glycerol) with freshly added dithiothreitol/DTT (1 mM), PMSF (100 μM) and protease inhibitor cocktail (Roche, Branford, CT). Cells were incubated for 30 minutes on ice and sonicated in Bioruptor Ultra-sonication system (Diagenode, Denville, NJ). SDS-PAGE sample buffer was added to sonicated extracts and boiled. Samples were resolved by SDS-PAGE and transferred to PVDF membranes (Millipore, Billerica, MA). Membranes were blotted with antibodies then visualized by Immobilon Western Chemiluminescent reagent (Millipore) using Bio-Rad ChemiDoc MP system (Bio-Rad, Hercules, CA). Antibodies used in this study: PRMT1 (Cat# 07404, Millipore), LDHA (Cat#MA5-17246, Invitrogen), p-LDHA (Cat# 8176, Cell Signaling), CPT1a (Cat#66039, Proteintech).

Quantitative Real-time PCR

Total RNA was prepared using Direct-Zol RNAprep Kit (Zymo research, Irvine, CA). cDNA was generated by the Verso cDNA synthesis Kit (Thermo Scientific, Walthum, MA) with random hexamer priming. Real-time PCR assays were performed with Absolute Blue qPCR SYBR green Mix (Thermo Scientific) on a ViiA 7 system (Applied Biosystems, Walthum, MA). Relative quantity of gene expression was calculated by the ΔΔCt method. Housekeeping gene beta-Actin was used for normalization.

Primer list:

Prmt1-F	CCCGTGGAGAAGGTGGACAT
Prmt1-R	CTCCCACCAGTGGATCTTGT
Cpt1a-F	GGCATAAACGCAGAGCATTCCTG
Cpt1a-R	CAGTGTCCATCCTCTGAGTAGC
Idha-F	GAATTACGATGGGGATGTGC
Idha-R	GACGTCTCTTGCCCTTTCTG
Fasn-F	AAGTTCGACGCCTCCTTTTT
Fasn-R	TGCCTCTGAACCACTCACAC

Cell Viability Assays

Cell viability was measured by using CellTiter-Glo Viability Assay Kit (Promega, Madison, WI). One

thousand 6133 cells were seeded in 96-well plates (100 μL per well) with or without treatment. At the indicated time post culture setup, 100 μL of CellTiter-Glo reagent was added into each well. The luminescent signal was measured using a microplate reader (Biotek, Winooski, VT).

Metabolite extraction

Cells were washed twice with ice-cold PBS, followed by metabolite extraction in −70 °C in a 20% methanol solution (LC-MS grade methanol, Fisher Scientific). The tissue–methanol mixture was subjected to bead-beating for 45 seconds using a Tissue/cell disrupter (Qiagen). Extracts were centrifuged for 5 min at 2000Xg to pellet insoluble material and supernatants were transferred to clean tubes. The extraction procedure was repeated two additional times and all three supernatants were pooled, dried in a Vacufuge (Eppendorf) and stored at −80 °C until analysis. The methanol-insoluble protein pellet was solubilized in 0.2 M NaOH at 95 °C for 20 min and protein was quantified using a BioRad DC assay. On the day of metabolite analysis, dried cell extracts were reconstituted in 70% acetonitrile at a relative protein concentration of 1 μg/ml, and 4 μl of this reconstituted extract was injected for LC/MS-based untargeted metabolite profiling.

LC/MS metabolomics

Cell extracts were analyzed by LC/MS platform comprised of an Agilent Model 1290 Infinity II liquid chromatography system coupled to an Agilent 6550 iFunnel time-of-flight MS analyzer. Chromatography of metabolites utilized aqueous normal phase (ANP) chromatography on a Diamond Hydride column (Microsolv). Mobile phases consisted of: (A) 50% isopropanol, containing 0.025% acetic acid, and (B) 90% acetonitrile containing 5 mM ammonium acetate. To eliminate the interference of metal ions on chromatographic peak integrity and electrospray ionization, EDTA was added to the mobile phase at a final concentration of 6 μM. The mobile phase gradient used was: 0–1.0 min, 99% B; 1.0–15.0 min, to 20% B; 15.0 to 29.0, 0% B; 29.1 to 37 min, 99% B. Raw data were analyzed using MassHunter Profinder 8.0 and MassProfiler Professional (MPP) 15.1 software (Agilent technologies).

Metabolite structure specification

To ascertain the identities of differentially expressed metabolites ($P < 0.05$), LC/MS data were searched against an in-house annotated personal metabolite database, created using MassHunter PCDL manager

8.0 (Agilent Technologies) based on monoisotopic neutral mass (<5 ppm mass accuracy) and chromatographic retention times of pure standards. A molecular formula generator (MFG) algorithm in MPP was used to generate and score empirical molecular formulae, based on a weighted consideration of monoisotopic mass accuracy, isotope abundance ratios, and spacing between isotope peaks. A tentative compound ID was assigned when the PCDL database and MFG scores concurred for a given candidate molecule. Tentatively assigned molecules were confirmed based on a match of LC retention times and/or MS/MS fragmentation spectra for pure molecular standards.

Seahorse Assays

Measurement of metabolic activities of leukemia cells was performed using the Seahorse XF24 analyzers (Agilent Technologies, Santa Clara, CA). 1.5-2 $x10^5$ cells per well were seeded in 24-well plate coated with Cell-Tal reagent (Corning, Corning NY). Assay started at basal condition, followed with Oligomycin (500nM), FCCP (5 µM) and antimycin A (1 µM) injected sequentially to culture.

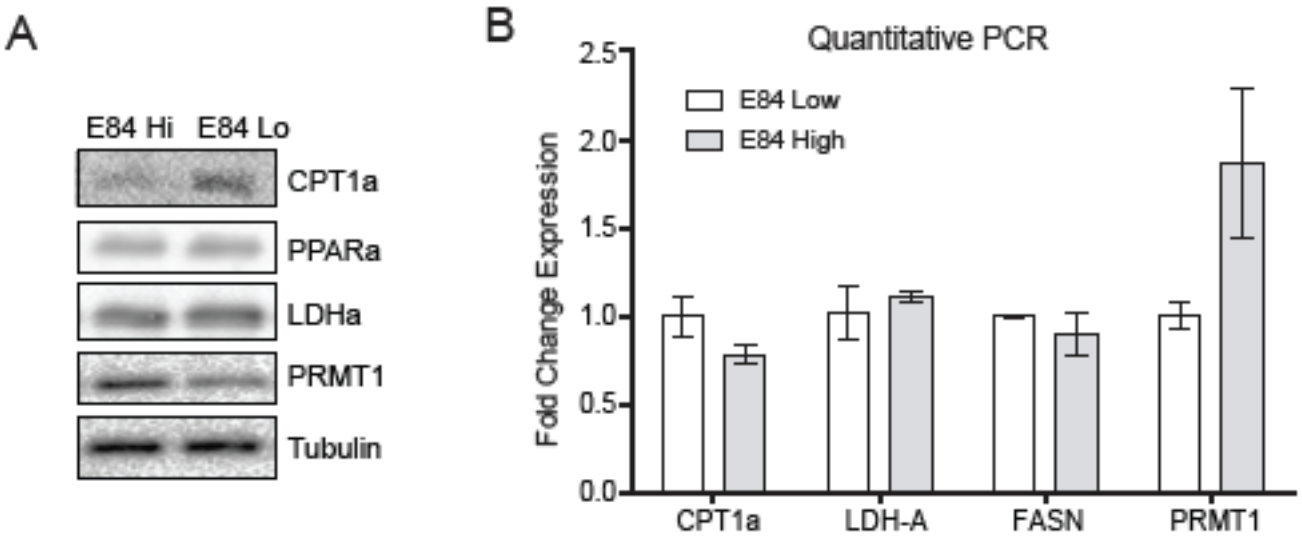

Supplemental Figure 1. Expression of metabolic regulated genes in cells with differential PRMT1 Expression levels.

A. Two populations of 6133 cells were FACS-sorted based on E84 staining intensity, as in Figure 1. Sorted cells were harvested and subjected to western blotting.

B. RNA was extracted from sorted cells and used for quantitative real-time PCR.

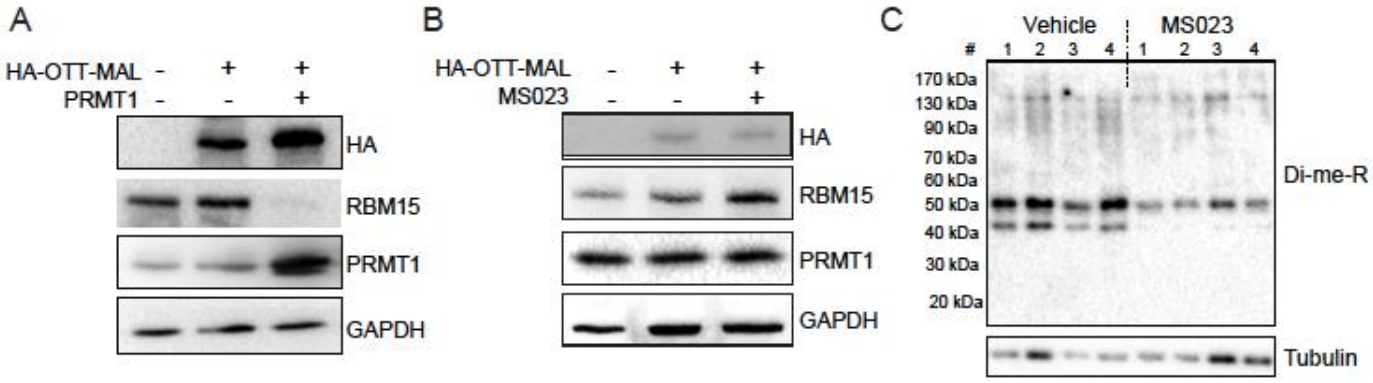

Supplemental Figure 2. RBM15-MKL1 (OTT-MAL) Protein Stability is not Affected by PRMT1 Activity.

A. HEK293T cells were transfected with constructs expressing HA-tagged RBM15-MKL1 with or without PRMT1. Extracts were harvested at 24 hours post transfection and then used for western blotting. Endogenous RBM15 is indicated.

B. NB4 cells were treated with PRMT1 inhibitor MS023 for 24 hours. Extracts were harvested for western blotting.

C. Global arginine di-methylation (Di-me-R) of bone marrow cells from mice injected with PRMT1 inhibitor MS023. Mice were injected with 80 mg/kg body weight of MS023 or vehicle every other day, for 30 days. Bone marrow cells were collected and extracts were prepared for western blotting.

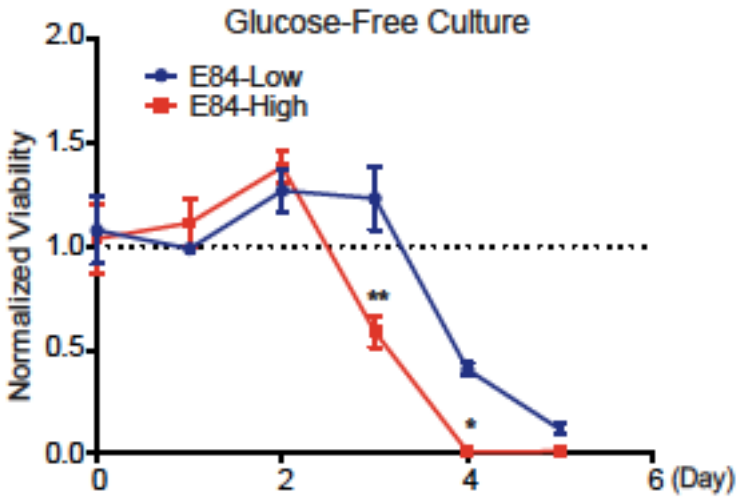

Supplemental Figure 3. Responsiveness to Glucose Restriction of Cells with Differential PRMT1 Expression levels. FACS-sorted E84-high and E84-low 6133 cells were washed with fresh medium and then seeded in glucose-free RPMI1640 medium for continuing culture. The viability of E84-high/low cells was measured by CellTiter-Glo assay.

References:

1. Kreitz, J., Schonfeld, C., Seibert, M., Stolp, V., Alshamleh, I., Oellerich, T., Steffen, B., Schwalbe, H., Schnutgen, F., Kurrle, N., and Serve, H. (2019). Metabolic Plasticity of Acute Myeloid Leukemia. Cells *8*. 10.3390/cells8080805.
2. Chen, W.L., Wang, J.H., Zhao, A.H., Xu, X., Wang, Y.H., Chen, T.L., Li, J.M., Mi, J.Q., Zhu, Y.M., Liu, Y.F., et al. (2014). A distinct glucose metabolism signature of acute myeloid leukemia with prognostic value. Blood *124*, 1645-1654. 10.1182/blood-2014-02-554204.
3. Lagadinou, E.D., Sach, A., Callahan, K., Rossi, R.M., Neering, S.J., Minhajuddin, M., Ashton, J.M., Pei, S., Grose, V., O'Dwyer, K.M., et al. (2013). BCL-2 inhibition targets oxidative phosphorylation and selectively eradicates quiescent human leukemia stem cells. Cell Stem Cell *12*, 329-341. 10.1016/j.stem.2012.12.013.
4. Jones, C.L., Stevens, B.M., D'Alessandro, A., Reisz, J.A., Culp-Hill, R., Nemkov, T., Pei, S., Khan, N., Adane, B., Ye, H., et al. (2019). Inhibition of Amino Acid Metabolism Selectively Targets Human Leukemia Stem Cells. Cancer Cell *35*, 333-335. 10.1016/j.ccell.2019.01.013.
5. Faubert, B., Solmonson, A., and DeBerardinis, R.J. (2020). Metabolic reprogramming and cancer progression. Science *368*. 10.1126/science.aaw5473.
6. L, M.G., Boulay, K., Topisirovic, I., Huot, M.E., and Mallette, F.A. (2017). Oncogenic Activities of IDH1/2 Mutations: From Epigenetics to Cellular Signaling. Trends Cell Biol *27*, 738-752. 10.1016/j.tcb.2017.06.002.
7. Choi, D., Oh, K.J., Han, H.S., Yoon, Y.S., Jung, C.Y., Kim, S.T., and Koo, S.H. (2012). Protein arginine methyltransferase 1 regulates hepatic glucose production in a FoxO1-dependent manner. Hepatology *56*, 1546-1556. 10.1002/hep.25809.
8. Laplante, M., and Sabatini, D.M. (2013). Regulation of mTORC1 and its impact on gene expression at a glance. J Cell Sci *126*, 1713-1719. 10.1242/jcs.125773.
9. Humpton, T.J., Hock, A.K., Maddocks, O.D.K., and Vousden, K.H. (2018). p53-mediated adaptation to serine starvation is retained by a common tumour-derived mutant. Cancer Metab *6*, 18. 10.1186/s40170-018-0191-6.
10. Schwartzenberg-Bar-Yoseph, F., Armoni, M., and Karnieli, E. (2004). The tumor suppressor p53 down-regulates glucose transporters GLUT1 and GLUT4 gene expression. Cancer Res *64*, 2627-2633. 10.1158/0008-5472.can-03-0846.
11. Ferrer, C.M., Lynch, T.P., Sodi, V.L., Falcone, J.N., Schwab, L.P., Peacock, D.L., Vocadlo, D.J., Seagroves, T.N., and Reginato, M.J. (2014). O-GlcNAcylation regulates cancer metabolism and survival stress signaling via regulation of the HIF-1 pathway. Mol Cell *54*, 820-831. 10.1016/j.molcel.2014.04.026.
12. Kalaitzidis, D., Sykes, S.M., Wang, Z., Punt, N., Tang, Y., Ragu, C., Sinha, A.U., Lane, S.W., Souza, A.L., Clish, C.B., et al. (2012). mTOR complex 1 plays critical roles in hematopoiesis and Pten-loss-evoked leukemogenesis. Cell Stem Cell *11*, 429-439. 10.1016/j.stem.2012.06.009.
13. Zhao, X., Jankovic, V., Gural, A., Huang, G., Pardanani, A., Menendez, S., Zhang, J., Dunne, R., Xiao, A., Erdjument-Bromage, H., et al. (2008). Methylation of RUNX1 by PRMT1 abrogates SIN3A binding and potentiates its transcriptional activity. Genes Dev *22*, 640-653. 10.1101/gad.1632608.
14. Wang, H., Huang, Z.Q., Xia, L., Feng, Q., Erdjument-Bromage, H., Strahl, B.D., Briggs, S.D., Allis, C.D., Wong, J., Tempst, P., and Zhang, Y. (2001). Methylation of histone H4 at arginine 3

511 facilitating transcriptional activation by nuclear hormone receptor. Science *293*, 853-857.
512 10.1126/science.1060781.
513 15. Baldwin, R.M., Morettin, A., Paris, G., Goulet, I., and Cote, J. (2012). Alternatively spliced protein
514 arginine methyltransferase 1 isoform PRMT1v2 promotes the survival and invasiveness of
515 breast cancer cells. Cell Cycle *11*, 4597-4612. 10.4161/cc.22871.
516 16. Cho, E.C., Zheng, S., Munro, S., Liu, G., Carr, S.M., Moehlenbrink, J., Lu, Y.C., Stimson, L., Khan, O.,
517 Konietzny, R., et al. (2012). Arginine methylation controls growth regulation by E2F-1. The
518 EMBO journal *31*, 1785-1797. 10.1038/emboj.2012.17.
519 17. Cho, J.H., Lee, M.K., Yoon, K.W., Lee, J., Cho, S.G., and Choi, E.J. (2012). Arginine methylation-
520 dependent regulation of ASK1 signaling by PRMT1. Cell Death Differ *19*, 859-870.
521 10.1038/cdd.2011.168.
522 18. Guendel, I., Carpio, L., Pedati, C., Schwartz, A., Teal, C., Kashanchi, F., and Kehn-Hall, K. (2010).
523 Methylation of the tumor suppressor protein, BRCA1, influences its transcriptional cofactor
524 function. PloS one *5*, e11379. 10.1371/journal.pone.0011379.
525 19. Karkhanis, V., Hu, Y.J., Baiocchi, R.A., Imbalzano, A.N., and Sif, S. (2011). Versatility of PRMT5-
526 induced methylation in growth control and development. Trends in biochemical sciences.
527 10.1016/j.tibs.2011.09.001.
528 20. Le Romancer, M., Treilleux, I., Leconte, N., Robin-Lespinasse, Y., Sentis, S., Bouchekioua-
529 Bouzaghou, K., Goddard, S., Gobert-Gosse, S., and Corbo, L. (2008). Regulation of estrogen rapid
530 signaling through arginine methylation by PRMT1. Mol Cell *31*, 212-221.
531 10.1016/j.molcel.2008.05.025.
532 21. Mitchell, T.R., Glenfield, K., Jeyanthan, K., and Zhu, X.D. (2009). Arginine methylation regulates
533 telomere length and stability. Mol Cell Biol *29*, 4918-4934. 10.1128/mcb.00009-09.
534 22. Yang, Y., and Bedford, M.T. (2013). Protein arginine methyltransferases and cancer. Nature
535 reviews. Cancer *13*, 37-50. 10.1038/nrc3409.
536 23. Yoshimatsu, M., Toyokawa, G., Hayami, S., Unoki, M., Tsunoda, T., Field, H.I., Kelly, J.D., Neal,
537 D.E., Maehara, Y., Ponder, B.A., et al. (2011). Dysregulation of PRMT1 and PRMT6, Type I
538 arginine methyltransferases, is involved in various types of human cancers. Int J Cancer *128*,
539 562-573. 10.1002/ijc.25366.
540 24. Avasarala, S., Van Scoyk, M., Karuppusamy Rathinam, M.K., Zerayesus, S., Zhao, X., Zhang, W.,
541 Pergande, M.R., Borgia, J.A., DeGregori, J., Port, J.D., et al. (2015). PRMT1 is a Novel Regulator of
542 Epithelial-Mesenchymal-Transition in Non-Small Cell Lung Cancer. J Biol Chem.
543 10.1074/jbc.M114.636050.
544 25. Lin, W.J., Gary, J.D., Yang, M.C., Clarke, S., and Herschman, H.R. (1996). The mammalian
545 immediate-early TIS21 protein and the leukemia-associated BTG1 protein interact with a
546 protein-arginine N-methyltransferase. J Biol Chem *271*, 15034-15044.
547 26. Shia, W.J., Okumura, A.J., Yan, M., Sarkeshik, A., Lo, M.C., Matsuura, S., Komeno, Y., Zhao, X.,
548 Nimer, S.D., Yates, J.R., 3rd, and Zhang, D.E. (2012). PRMT1 interacts with AML1-ETO to
549 promote its transcriptional activation and progenitor cell proliferative potential. Blood *119*,
550 4953-4962. 10.1182/blood-2011-04-347476.
551 27. Cheung, N., Chan, L.C., Thompson, A., Cleary, M.L., and So, C.W. (2007). Protein arginine-
552 methyltransferase-dependent oncogenesis. Nature cell biology *9*, 1208-1215.
553 10.1038/ncb1642.
554 28. Zou, L., Zhang, H., Du, C., Liu, X., Zhu, S., Zhang, W., Li, Z., Gao, C., Zhao, X., Mei, M., et al. (2012).
555 Correlation of SRSF1 and PRMT1 expression with clinical status of pediatric acute
556 lymphoblastic leukemia. Journal of hematology & oncology *5*, 42. 10.1186/1756-8722-5-42.

557 29. He, X., Zhu, Y., Lin, Y.C., Li, M., Du, J., Dong, H., Sun, J., Zhu, L., Wang, H., Ding, Z., et al. (2019).
558 PRMT1-mediated FLT3 arginine methylation promotes maintenance of FLT3-ITD(+) acute
559 myeloid leukemia. Blood *134*, 548-560. 10.1182/blood.2019001282.
560 30. Fong, J.Y., Pignata, L., Goy, P.A., Kawabata, K.C., Lee, S.C., Koh, C.M., Musiani, D., Massignani, E.,
561 Kotini, A.G., Penson, A., et al. (2019). Therapeutic Targeting of RNA Splicing Catalysis through
562 Inhibition of Protein Arginine Methylation. Cancer cell *36*, 194-209 e199.
563 10.1016/j.ccell.2019.07.003.
564 31. Butcher, R.A., Bhullar, B.S., Perlstein, E.O., Marsischky, G., LaBaer, J., and Schreiber, S.L. (2006).
565 Microarray-based method for monitoring yeast overexpression strains reveals small-molecule
566 targets in TOR pathway. Nat Chem Biol *2*, 103-109. 10.1038/nchembio762.
567 32. Messier, V., Zenklusen, D., and Michnick, S.W. (2013). A nutrient-responsive pathway that
568 determines M phase timing through control of B-cyclin mRNA stability. Cell *153*, 1080-1093.
569 10.1016/j.cell.2013.04.035.
570 33. Sha, L., Daitoku, H., Araoi, S., Kaneko, Y., Takahashi, Y., Kako, K., and Fukamizu, A. (2016).
571 Asymmetric Arginine Dimethylation Modulates Mitochondrial Energy Metabolism and
572 Homeostasis in Caenorhabditis elegans. Molecular and cellular biology. 10.1128/mcb.00504-
573 16.
574 34. Fisk, J.C., and Read, L.K. (2011). Protein arginine methylation in parasitic protozoa. Eukaryotic
575 cell *10*, 1013-1022. 10.1128/ec.05103-11.
576 35. Kafkova, L., Tu, C., Pazzo, K.L., Smith, K.P., Debler, E.W., Paul, K.S., Qu, J., and Read, L.K. (2018).
577 Trypanosoma brucei PRMT1 Is a Nucleic Acid Binding Protein with a Role in Energy
578 Metabolism and the Starvation Stress Response. MBio *9*. 10.1128/mBio.02430-18.
579 36. Athale, U.H., Razzouk, B.I., Raimondi, S.C., Tong, X., Behm, F.G., Head, D.R., Srivastava, D.K.,
580 Rubnitz, J.E., Bowman, L., Pui, C.H., and Ribeiro, R.C. (2001). Biology and outcome of childhood
581 acute megakaryoblastic leukemia: a single institution's experience. Blood *97*, 3727-3732.
582 37. Ma, Z., Morris, S.W., Valentine, V., Li, M., Herbrick, J.A., Cui, X., Bouman, D., Li, Y., Mehta, P.K.,
583 Nizetic, D., et al. (2001). Fusion of two novel genes, RBM15 and MKL1, in the t(1;22)(p13;q13)
584 of acute megakaryoblastic leukemia. Nat Genet *28*, 220-221. 10.1038/90054.
585 38. Mercher, T., Coniat, M.B., Monni, R., Mauchauffe, M., Nguyen Khac, F., Gressin, L., Mugneret, F.,
586 Leblanc, T., Dastugue, N., Berger, R., and Bernard, O.A. (2001). Involvement of a human gene
587 related to the Drosophila spen gene in the recurrent t(1;22) translocation of acute
588 megakaryocytic leukemia. Proc Natl Acad Sci U S A *98*, 5776-5779. 10.1073/pnas.101001498.
589 39. Zhu, Y., He, X., Lin, Y.C., Dong, H., Zhang, L., Chen, X., Wang, Z., Shen, Y., Li, M., Wang, H., et al.
590 (2019). Targeting PRMT1-mediated FLT3 methylation disrupts maintenance of MLL-
591 rearranged acute lymphoblastic leukemia. Blood *134*, 1257-1268. 10.1182/blood.2019002457.
592 40. Zhang, L., Tran, N.T., Su, H., Wang, R., Lu, Y., Tang, H., Aoyagi, S., Guo, A., Khodadadi-Jamayran,
593 A., Zhou, D., et al. (2015). Cross-talk between PRMT1-mediated methylation and ubiquitylation
594 on RBM15 controls RNA splicing. Elife *4*, e07938. 10.7554/eLife.07938.
595 41. Su, H., Jiang, M., Senevirathne, C., Aluri, S., Zhang, T., Guo, H., Xavier-Ferrucio, J., Jin, S., Tran,
596 N.T., Liu, S.M., et al. (2021). Methylation of dual-specificity phosphatase 4 controls cell
597 differentiation. Cell Rep *36*, 109421. 10.1016/j.celrep.2021.109421.
598 42. Mercher, T., Raffel, G.D., Moore, S.A., Cornejo, M.G., Baudry-Bluteau, D., Cagnard, N., Jesneck, J.L.,
599 Pikman, Y., Cullen, D., Williams, I.R., et al. (2009). The OTT-MAL fusion oncogene activates
600 RBPJ-mediated transcription and induces acute megakaryoblastic leukemia in a knockin
601 mouse model. The Journal of clinical investigation *119*, 852-864. 10.1172/jci35901.

602 43. Su, H., Sun, C.W., Liu, S.M., He, X., Hu, H., Pawlik, K.M., Townes, T.M., Han, X., Klug, C.A., Henary,
603 M., et al. (2018). Defining the epigenetic status of blood cells using a cyanine-based fluorescent
604 probe for PRMT1. Blood Adv *2*, 2829-2836. 10.1182/bloodadvances.2018020727.
605 44. Thiollier, C., Lopez, C.K., Gerby, B., Ignacimouttou, C., Poglio, S., Duffourd, Y., Guegan, J., Rivera-
606 Munoz, P., Bluteau, O., Mabialah, V., et al. (2012). Characterization of novel genomic alterations
607 and therapeutic approaches using acute megakaryoblastic leukemia xenograft models. J Exp
608 Med *209*, 2017-2031. 10.1084/jem.20121343.
609 45. Eram, M.S., Shen, Y., Szewczyk, M.M., Wu, H., Senisterra, G., Li, F., Butler, K.V., Kaniskan, H.U.,
610 Speed, B.A., dela Sena, C., et al. (2016). A Potent, Selective, and Cell-Active Inhibitor of Human
611 Type I Protein Arginine Methyltransferases. ACS Chem Biol *11*, 772-781.
612 10.1021/acschembio.5b00839.
613 46. Divakaruni, A.S., Paradyse, A., Ferrick, D.A., Murphy, A.N., and Jastroch, M. (2014). Analysis and
614 interpretation of microplate-based oxygen consumption and pH data. Methods Enzymol *547*,
615 309-354. 10.1016/b978-0-12-801415-8.00016-3.
616 47. Fan, J., Hitosugi, T., Chung, T.W., Xie, J., Ge, Q., Gu, T.L., Polakiewicz, R.D., Chen, G.Z., Boggon, T.J.,
617 Lonial, S., et al. (2011). Tyrosine phosphorylation of lactate dehydrogenase A is important for
618 NADH/NAD(+) redox homeostasis in cancer cells. Molecular and cellular biology *31*, 4938-
619 4950. 10.1128/MCB.06120-11.
620 48. Pang, Z., Lu, Y., Zhou, G., Hui, F., Xu, L., Viau, C., Spigelman, A.F., MacDonald, P.E., Wishart, D.S.,
621 Li, S., and Xia, J. (2024). MetaboAnalyst 6.0: towards a unified platform for metabolomics data
622 processing, analysis and interpretation. Nucleic Acids Res *52*, W398-W406.
623 10.1093/nar/gkae253.
624 49. Menendez, J.A., and Lupu, R. (2007). Fatty acid synthase and the lipogenic phenotype in cancer
625 pathogenesis. Nature reviews. Cancer *7*, 763-777. 10.1038/nrc2222.
626 50. Samudio, I., Harmancey, R., Fiegl, M., Kantarjian, H., Konopleva, M., Korchin, B., Kaluarachchi, K.,
627 Bornmann, W., Duvvuri, S., Taegtmeyer, H., and Andreeff, M. (2010). Pharmacologic inhibition
628 of fatty acid oxidation sensitizes human leukemia cells to apoptosis induction. The Journal of
629 clinical investigation *120*, 142-156. 10.1172/jci38942.
630 51. Kurmi, K., Hitosugi, S., Wiese, E.K., Boakye-Agyeman, F., Gonsalves, W.I., Lou, Z., Karnitz, L.M.,
631 Goetz, M.P., and Hitosugi, T. (2018). Carnitine Palmitoyltransferase 1A Has a Lysine
632 Succinyltransferase Activity. Cell Rep *22*, 1365-1373. 10.1016/j.celrep.2018.01.030.
633 52. Cho, J.H., Lee, R., Kim, E., Choi, Y.E., and Choi, E.J. (2018). PRMT1 negatively regulates
634 activation-induced cell death in macrophages by arginine methylation of GAPDH. Exp Cell Res
635 *368*, 50-58. 10.1016/j.yexcr.2018.04.012.
636 53. Wang, K., Luo, L., Fu, S., Wang, M., Wang, Z., Dong, L., Wu, X., Dai, L., Peng, Y., Shen, G., et al.
637 (2023). PHGDH arginine methylation by PRMT1 promotes serine synthesis and represents a
638 therapeutic vulnerability in hepatocellular carcinoma. Nat Commun *14*, 1011.
639 10.1038/s41467-023-36708-5.
640 54. Goulah, C.C., Pelletier, M., and Read, L.K. (2006). Arginine methylation regulates mitochondrial
641 gene expression in Trypanosoma brucei through multiple effector proteins. RNA *12*, 1545-
642 1555. 10.1261/rna.90106.
643 55. Teyssier, C., Ma, H., Emter, R., Kralli, A., and Stallcup, M.R. (2005). Activation of nuclear
644 receptor coactivator PGC-1alpha by arginine methylation. Genes Dev *19*, 1466-1473.
645 56. Yamagata, K., Daitoku, H., Takahashi, Y., Namiki, K., Hisatake, K., Kako, K., Mukai, H., Kasuya, Y.,
646 and Fukamizu, A. (2008). Arginine methylation of FOXO transcription factors inhibits their
647 phosphorylation by Akt. Mol Cell *32*, 221-231. 10.1016/j.molcel.2008.09.013.

648 57. Xiao, N., Jani, K., Morgan, K., Okabe, R., Cullen, D.E., Jesneck, J.L., and Raffel, G.D. (2012).
649 Hematopoietic stem cells lacking Ott1 display aspects associated with aging and are unable to
650 maintain quiescence during proliferative stress. Blood *119*, 4898-4907. 10.1182/blood-2012-
651 01-403089.
652 58. Niu, C., Zhang, J., Breslin, P., Onciu, M., Ma, Z., and Morris, S.W. (2009). c-Myc is a target of RNA-
653 binding motif protein 15 in the regulation of adult hematopoietic stem cell and megakaryocyte
654 development. Blood *114*, 2087-2096. 10.1182/blood-2009-01-197921.
655 59. Birsoy, K., Wang, T., Chen, W.W., Freinkman, E., Abu-Remaileh, M., and Sabatini, D.M. (2015). An
656 Essential Role of the Mitochondrial Electron Transport Chain in Cell Proliferation Is to Enable
657 Aspartate Synthesis. Cell *162*, 540-551. 10.1016/j.cell.2015.07.016.
658 60. Sullivan, L.B., Gui, D.Y., Hosios, A.M., Bush, L.N., Freinkman, E., and Vander Heiden, M.G. (2015).
659 Supporting Aspartate Biosynthesis Is an Essential Function of Respiration in Proliferating
660 Cells. Cell *162*, 552-563. 10.1016/j.cell.2015.07.017.
661 61. Liu, L., Zhang, K., Sandoval, H., Yamamoto, S., Jaiswal, M., Sanz, E., Li, Z., Hui, J., Graham, B.H.,
662 Quintana, A., and Bellen, H.J. (2015). Glial lipid droplets and ROS induced by mitochondrial
663 defects promote neurodegeneration. Cell *160*, 177-190. 10.1016/j.cell.2014.12.019.

664